PROGRESS IN RADIO NEUTRINO DETECTION WITH ARIANNA

Conference on the Intersection of Nuclear and Particle Physics, 2015, Vail, CO. May 19-24

Jordan C. Hanson (j529h838@ku.edu, 918particle@gmail.com)

May 20, 2015

University of Kansas, Department of Physics and Astronomy

INTRODUCTION

Introduction

I. UHE Neutrinos, Askaryan Effect
   A. Cosmic rays and the GZK effect
   B. Askaryan effect, LPM corrections
II. Deployed Hardware
   A. Hardware used in this analysis
   B. Future hardware
   C. Timeline for future deployment
III. Ice
   A. Completed Research
   B. Future Research
IV. System Response
   A. Antenna Response
   B. Additional components
   C. Reflections, Modifications, Filtering
V. Data Analysis
   A. Expected signal, cuts
   B. Acquired Data
VI. Neutrino Sensitivity
   A. Flux-limit methodology
   B. Comparison to IceCube, pushing bounds further

Papers Covered

Time-Domain Response of the ARIANNA Detector

http://arxiv.org/abs/1406.0820.

Radar Absorption, Basal Reflection, Thickness, and Polarization Measurements from the Ross Ice Shelf

http://arxiv.org/abs/1410.7134.

A First Search for Cosmogenic Neutrinos with the ARIANNA Hexagonal Radio Array

http://arxiv.org/abs/1410.7352.

Design and Performance of the ARIANNA Hexagonal Radio Array Systems

http://arxiv.org/abs/1410.7369.

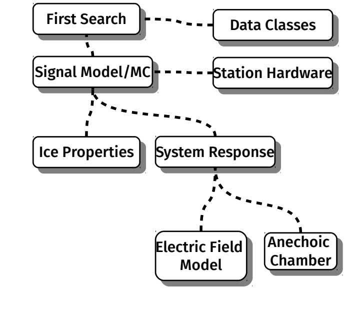

These papers have all been approved for publication, with the exception of http://arxiv.org/abs/1410.7369 (waiting to hear from reviewers). All have passed collaboration review.

UHE NEUTRINOS, ASKARYAN EFFECT

Cosmic rays produce large EAS, difficult to discern point sources and learn about HEP

I. Termination of the spectrum of cosmic rays has been observed (Salamida, 2011)
II. Difficult to distinguish point sources, even at high rigidity
III. Sources limited to $\approx$ 50 Mpc, via several energy loss mechanisms

Corresponding ν's make it easy to discern point sources and learn about HEP, but rarely interact.

I. Predictions for $dN_\nu/dE \approx E^{-2}$, low overall flux
II. Cosmological distribution of UHECR sources (IceCube - first constraints)

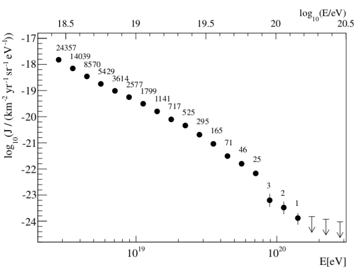

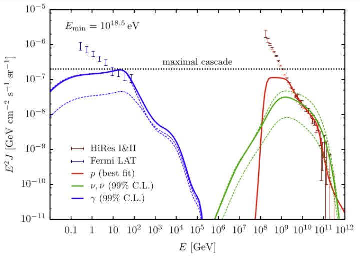

(Ahlers *et al.*, 2010).

Variety of Constraints

I. Cosmological permutations, including source evolution
II. Other particle messengers ($e^{\pm}$, γ)
III. Atomic number of cosmic rays (composition)...TA/Auger

$$\Phi_\nu = NG(z)E^{-\alpha}e^{-E/E_{max}} \quad (1)$$

$$G(z) = H(z)\frac{dt}{dz}\Phi_0 \quad (2)$$

```
Constraints:
    {H(0) = 1}
    {rho(z) = H(z)rho(0)}
    {H(z) = (1+z)^m, z<z_{max}}
    {H(z) = 0, z>z_{max}}
```

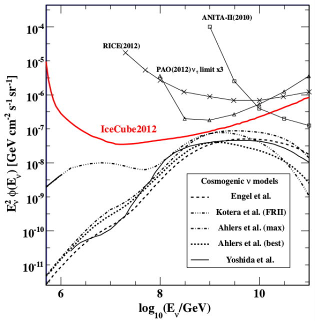

Eliminates upper line of pure protonic model, e.g. Kalashev *et al.*, with $m = 5$, $z_{max} = 3$. (Aartsen, 2013).

$$p^+ + \gamma_{CMB} \rightarrow \Delta^+ \rightarrow \pi^+ + n \quad (3)$$

$$\rightarrow \pi^0 + p^+ \quad (4)$$

$$\pi^+ \rightarrow e^+ + \nu_\mu + \nu_e + \bar{\nu}_\mu \quad (5)$$

$$\pi^0 \rightarrow \gamma\gamma \quad (6)$$

Askaryan Effect, Hadronic and Electromagnetic

- Shower created by the UHE-ν interaction radiates coherently in the GHz RF regime
- Had. and EM. showers have different depth-dependencies.
- Cerenkov angle, retarded time
- Electric field should be derivable from first principles (Ralston and Buniy, 2001).

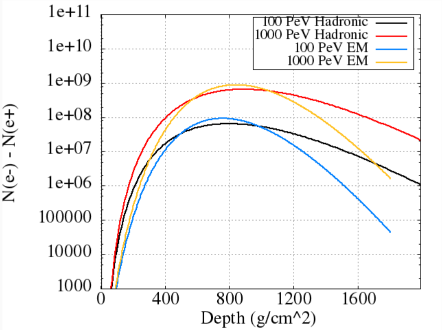

$$c\vec{A}_\omega(\vec{x}) = \int d^3\vec{x'} \frac{\exp\left(ik|\vec{x}-\vec{x'}|\right)}{|\vec{x}-\vec{x'}|} \int dt' \exp\left(i\omega t'\right)\vec{J}(t',\vec{x'}) \quad (7)$$

$$\vec{J}(t',\vec{x'}) = \vec{v}n(z')f(z'-vt',\vec{\rho'}) \quad (8)$$

$\hat{r}$-component of $\vec{E}$.

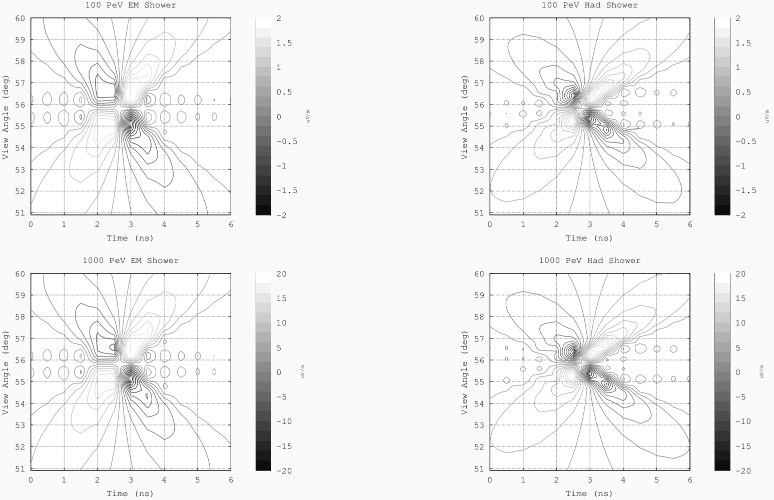

UHE Neutrinos, Askaryan Effect

$\hat{\theta}$-component of $\vec{E}$.

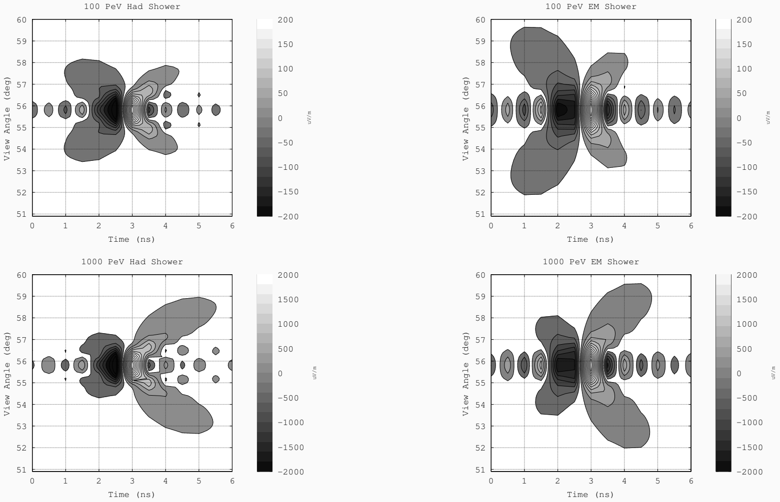

DEPLOYED HARDWARE

Stations are Radio Receivers

- Current stations - 4 antennas+amplifiers
- Future stations - 8 antennas+amplifiers
- Operate exclusively on solar power+batteries
- Micro-controller+comms: < 10 Watts

Analysis: 3/4 deployed stations in 2013

- Trigger: 2 of 4 antennas within 64 ns
- Combined live-time (stations A,C,G) of 170 days.
- Seven stations have now been deployed.
- Constitutes the full HRA (Hexagonal Radio Array)

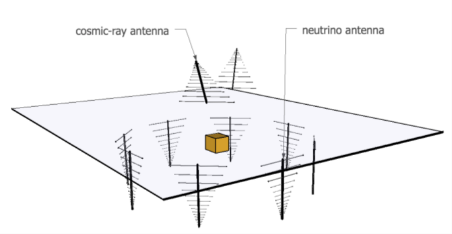

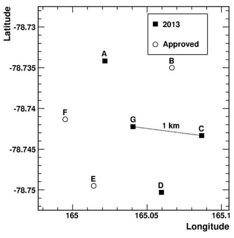

Array will be located in stable area

- 120 km to McMurdo station
- Far from man-made background sources
- Direct wifi-access infrastructure
- Satellite modem access
- Local ice flow does not affect ice purity
- Ice thickness over ocean forms fiducial volume

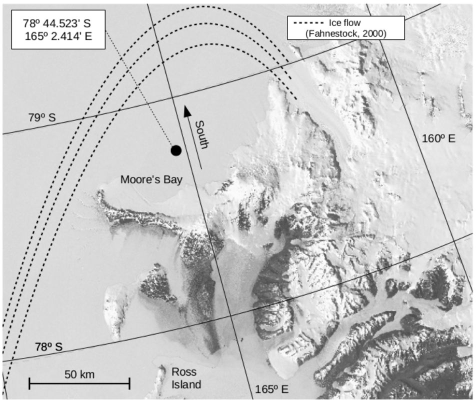

Objects in detection chain

- Log-periodic dipole array (LPDA)
- Low-noise amplifier (LNA)
- Filters, attenuators
- SST board (DAQ+trigger)

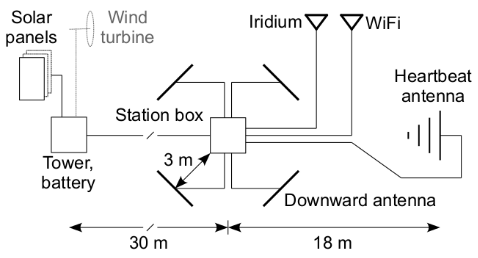

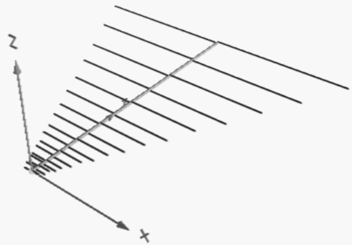

Objects in detection chain

- Log-periodic dipole array (LPDA)
- Low-noise amplifier (LNA)
- Filters, attenuators
- SST board (DAQ+trigger)

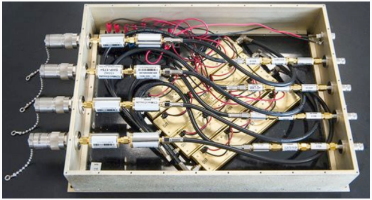

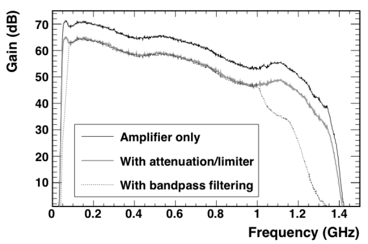

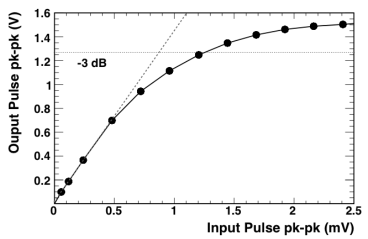

Objects in detection chain

- Log-periodic dipole array (LPDA)
- Low-noise amplifier (LNA)
- Filters, attenuators
- SST board (DAQ+trigger)

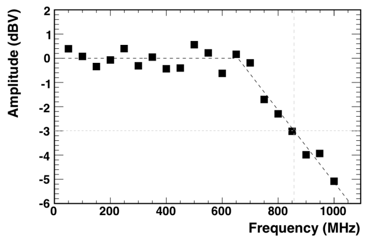

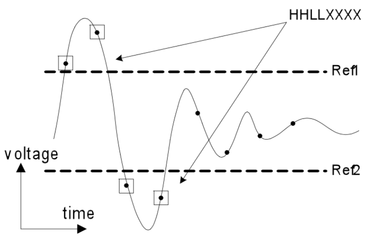

Objects in detection chain

- Log-periodic dipole array (LPDA)
- Low-noise amplifier (LNA)
- Filters, attenuators
- SST board (DAQ+trigger)

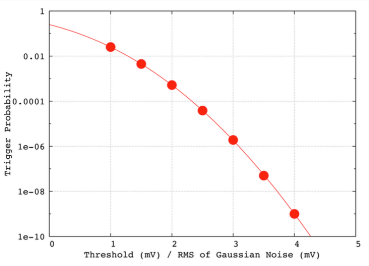

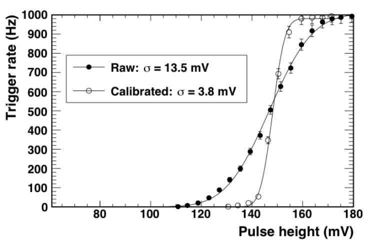

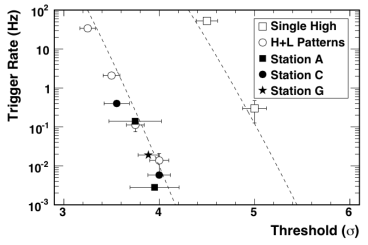

Improvements made to the DAQ, Future plans.

Prototype	2012-2014	Future
Bandwidth trigger	8-sample pattern	Common double threshold
2 freq. bands	72 patterns (HHLLXXXX...)	3 (H,L,HL)
4 channels	4 channels	8 channels
0 CR channels	0 CR channels	2 CR channels
30 Watts	10-20 Watts	7 Watts
Solar+Wind	Solar+Wind	Solar only
2.6 GHz sampling	1.92/2.0 GHz sampling	2.0 GHz sampling
Pb-acide AGM batt.	2×Li-ion batt.	Li-ion batt.

Timeline for full deployment:

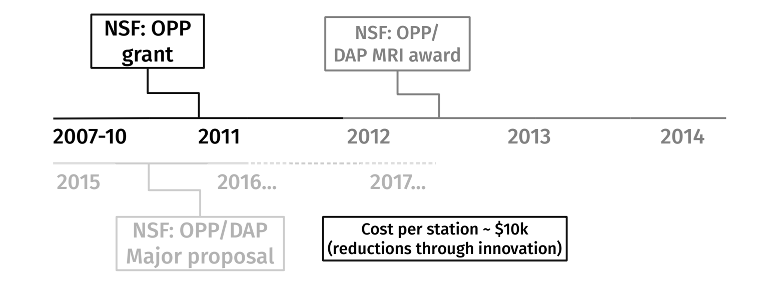

ICE

ICE

I. Ice
   A. Completed Research
      i. Ice thickness
      ii. RF Absoprtion of ice
      iii. Reflection coefficient
   B. Future Research
      i. Birefringence
      ii. Large scale (10 km) uniformity
      iii. Bore holes

Year	Δt_{meas}	Δt_{phys}	σ_{stat}	σ_{sys}	σ_{pulse}	σ_{tot}	d_{ice} (m)
2006	-	6783	-	-	-	10	577.5 ± 10
2009	-	6745	-	-	-	15	572 ± 6
2010	7060	6772	5.0	8.0	10	14	576 ± 6
2011	6964	6816	4.0	5.0	10	12	580 ± 6

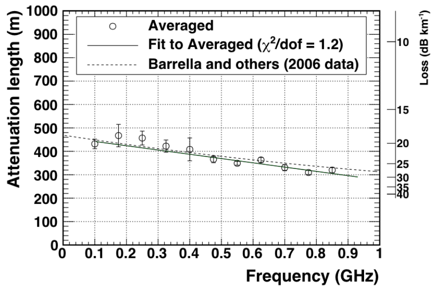

I. Ice
   A. Completed Research
      i. Ice thickness
      ii. RF Absoprtion of ice
      iii. Reflection coefficient
   B. Future Research
      i. Birefringence
      ii. Large scale (10 km) uniformity
      iii. Bore holes

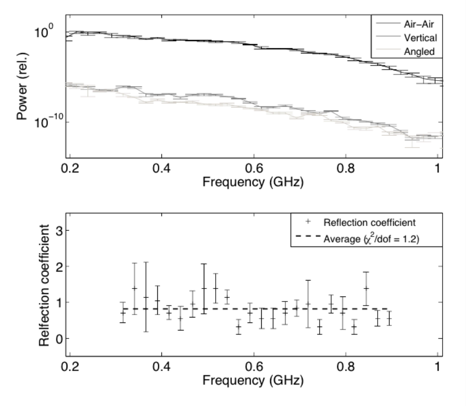

$\sqrt{R} = 0.82 \pm 0.07$. We will investigate different error assessments (doesn't affect strongly the fiducial volume).

SYSTEM RESPONSE

Askaryan pulse $\rightarrow$ data

LPDA converts electric field into voltage waveform

Voltage at LPDA terminal from E-field:

$$V_L(t) = 2\left(\frac{Z_L}{Z_L + Z_{in}}\right) h_{rx}(t) \circ E(t) \quad (9)$$

E-field from radiating LPDA:

$$E(r,t) = \frac{1}{2\pi rc}\left(\frac{Z_{in}}{Z_{in} + Z_L}\right)\left(\frac{Z_0}{Z_{in}}\right) h_{tx}(t) \circ V_{src}(t) \quad (10)$$

Combine, assuming impedance match (subtle, will return to this):

$$V_L(t) = \frac{1}{2\pi rc}\frac{Z_0}{Z_L} h_{rx} \circ h_{rx} \circ \dot{V}_{src}(t) \quad (11)$$

$$(h_{tx}(t) \equiv 2\dot{h}_{rx}(t)) \quad (12)$$

System Response

I. Derive the effective height
   A. Varying angle in *E*, *H-planes*
II. Incorporate transfer function of LNA
III. Test in anechoic chamber
IV. Test in the field
   A. **Includes ice effects**

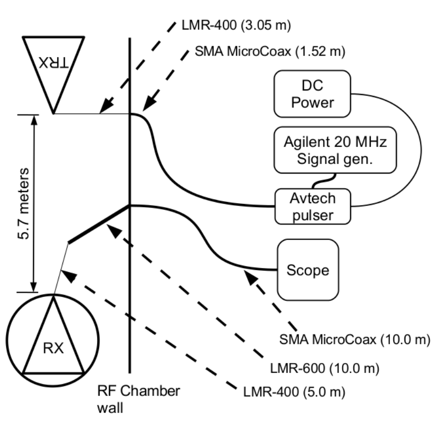

System Response

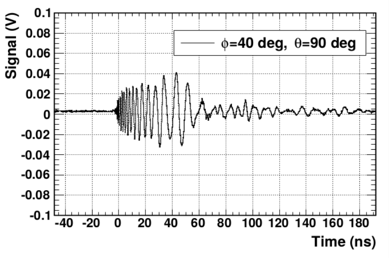

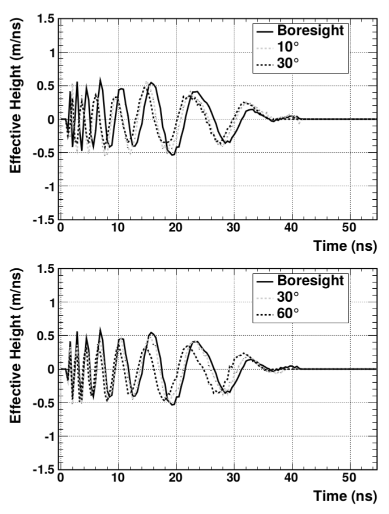

Data → solution

Using eq. 11, we find the solution for the effective height versus time. Repeat for all available E and H plane (fully covers main lobe).

System Response

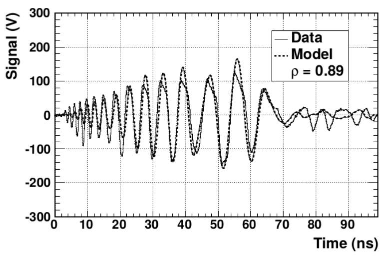

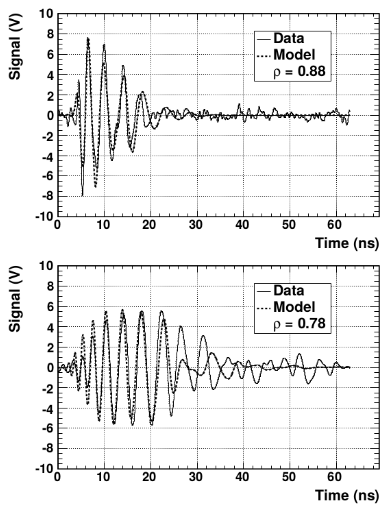

Predicting waveforms

Combining with measured *transfer function* of LNA, we can predict/model waveforms in the time-domain.

System Response

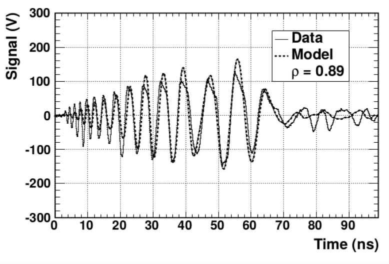

Exp. Setting	Fig.	ρ
Chamber+amplifier	11	0.89
Ice sounding (Moore's Bay 2006)	12	0.88
Ice sounding (Moore's Bay 2013)	12	0.78
In-air over ice (Moore's Bay 2012)	13	0.82
In-air (Aldrich Park (2010)	14	0.83

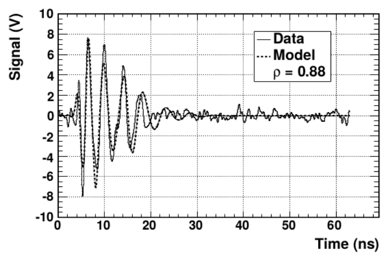

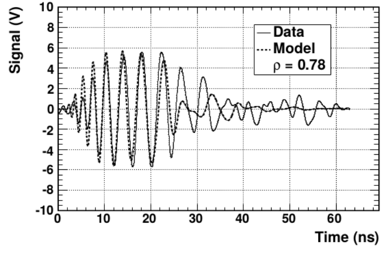

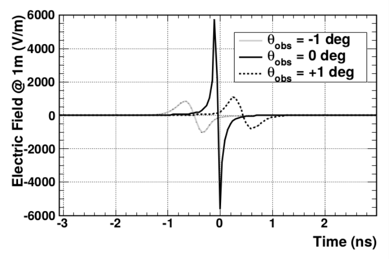

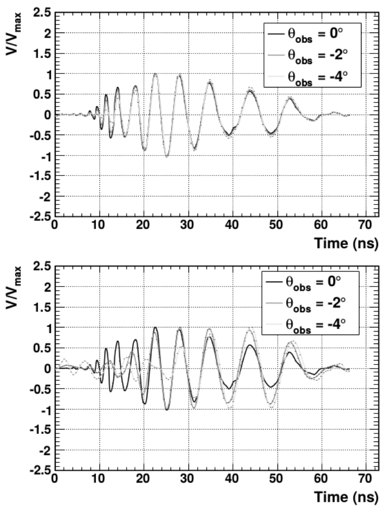

Predicting neutrino events

Combining all this information, we can create neutrino templates. We vary over E, H-planes, and observation angle. Energy, distance and ice absorption set the y-scale.

How can we improve this?

We determine the transfer function of remaining effects in multiple data sets, from data taken in 2013. This technique raises ρ to typically 0.7-0.8 (co-polarized cases).

Algorithm to determine additional effects

Use vector of small pseudo-random numbers in the Fourier domain to generate template iteration, and mimize the mean-square difference between data and model.

$$\vec{R_1}(\nu)' = \vec{R}(\nu) + \Re\vec{\epsilon}(\nu) \quad (13)$$

$$\vec{R_2}(\nu)' = \vec{R}(\nu) + \Im\vec{\epsilon}(\nu) \quad (14)$$

$$y_{1,2}(t) = \int r_{1,2}(\tau)s(t-\tau)d\tau \quad (15)$$

$$\mu^2 = |y_{1,2}(t) - d(t)|^2/n \quad (16)$$

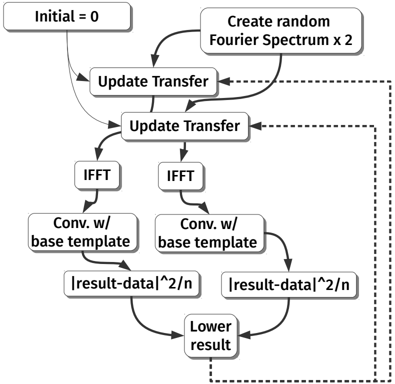

System Response

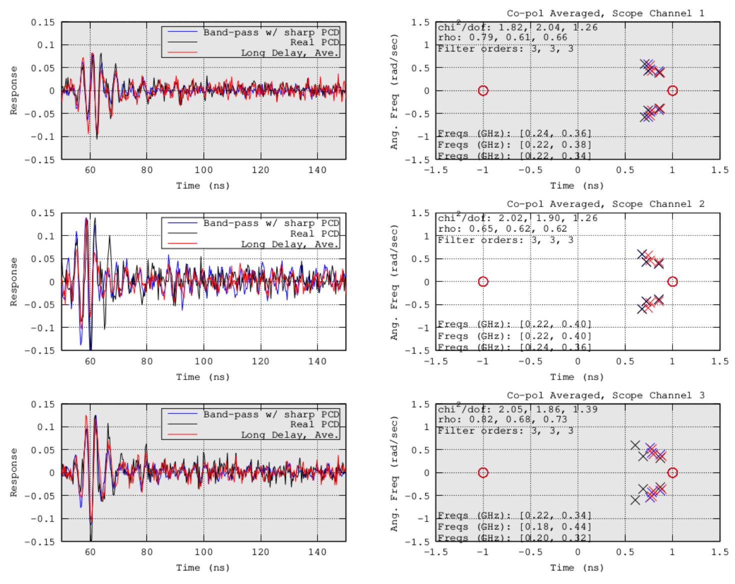

System Response

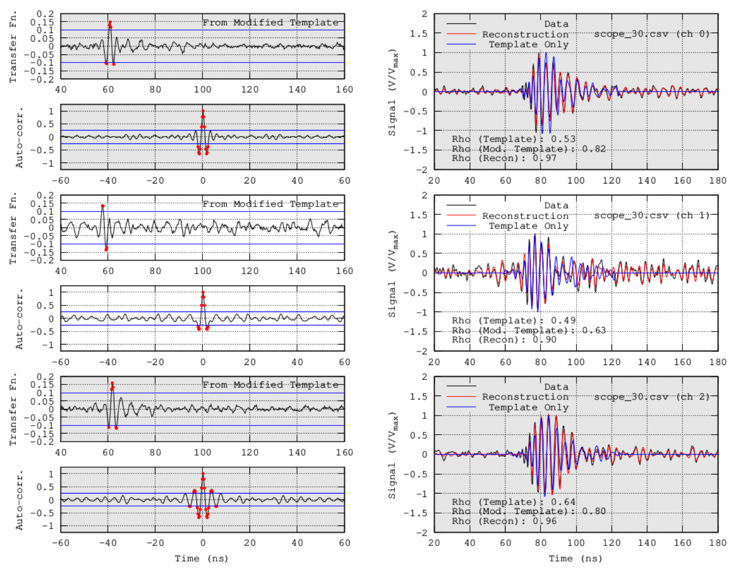

DATA ANALYSIS

Detector operations

Temperature effects required threshold adjustments. The event rate may be kept in the mHz regime, with thresholds of 4σ (with $\sigma = V_{rms}$ of unbiased events).

Classifying data

Three data classes: Thermal (biased) triggers, un-biased triggers, and heartbeats.

Three basic cuts

- α: Minimum auto-correlation value (<-0.45)
- η: Number of bins with at least half the power of the maximum bin in Fourier space (>3)
- χ: Maximum correlation value with neutrino template (among all channels, >0.81)

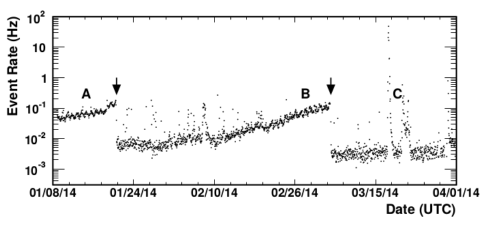

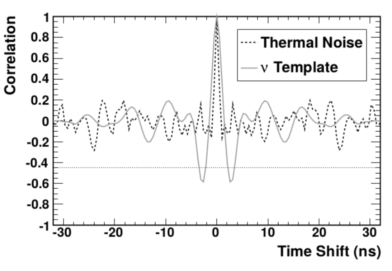

Three basic cuts

- α: Minimum auto-correlation value (<-0.45)
- η: Number of bins with at least half the power of the maximum bin in Fourier space (>3)
- χ: Maximum correlation value with neutrino template (among all channels, >0.81)

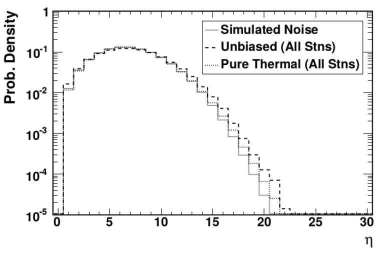

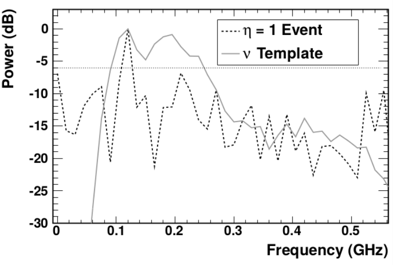

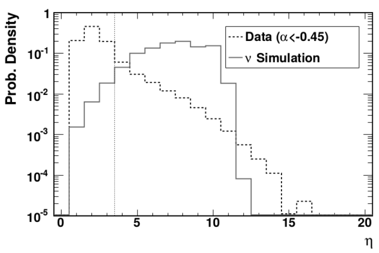

Three basic cuts

α: Minimum auto-correlation value (<-0.45)

η: Number of bins with at least half the power of the maximum bin in Fourier space (>3)

χ: Maximum correlation value with neutrino template (among all channels, >0.81)

Features

By selecting the best possible correlation of all *lags*, the simulated and un-biased distributions peak around ≈ 0.4, over 4 channels.

Feature near ≈ 0.68 in data is caused by high wind events (several potential causes)

Feature in signal MC near ≈ 0.7 caused by off-lobe events with respect to LPDA

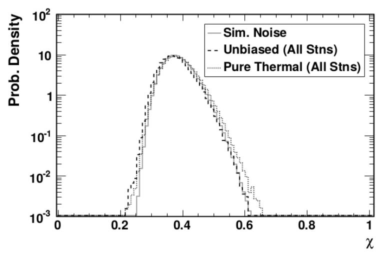

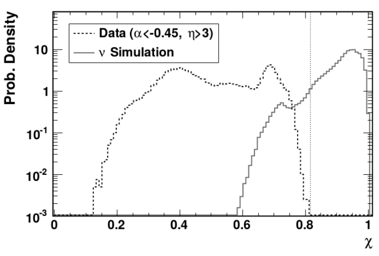

	Station A	Station G	Station C	All Data	Cosmogenic ν's
Triggers	203562	248772	512931	965265	100%
$\alpha < -0.45$	51327 (25%)	102599 (41%)	142243 (28%)	296169 (31%)	99.5%
$\eta > 3$	3159 (2%)	26868 (11%)	13461 (3%)	43488 (4.5%)	97%
$\chi > 0.81$	0 (0%)	0 (0%)	0 (0%)	0 (0%)	90%

Final cut table

- Final signal efficiency: 90%
- 965265 total events, 170 days combined live-time
- Threshold adjustments cause changes in number of α, η-passing events
- High-wind periods produce higher χ events.

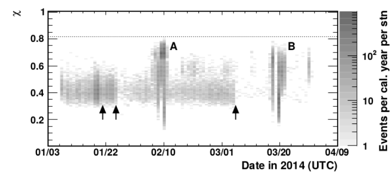

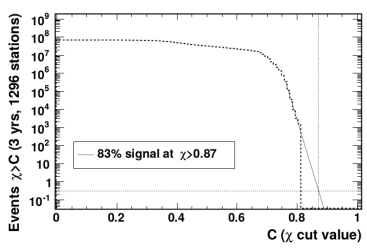

NEUTRINO SENSITIVITY

ARIANNA MC inherits from ANITA and RICE - still need LPM

Gal. coord., fraction of 1 yr.

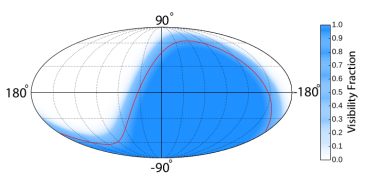

E_ν distribution.

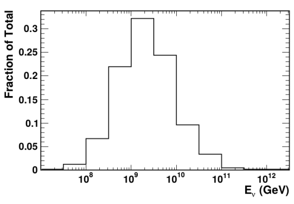

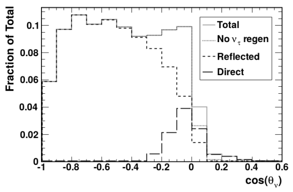

Zenith distribution.

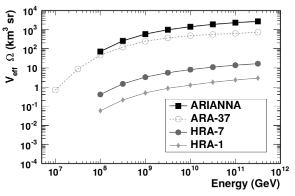

Effective volume.

Predicting neutrino events

Combining knowledge of ice, neutrino cross-section, geometry, and station design, we calculate the number of expected neutrino events in 3 years of observation.

Comparison to IceCube

The goal of the final design is to improve on the sensitivity of IceCube UHE analysis.

Neutrino Model	Model Type	N_ν Triggers ($E_\nu > 10^8$ GeV)	
		ARIANNA	IceCube [13]
ESS (2001) [38]	$m=4$, $\Omega_M=1$	55	
WB (1999) [66]	E_ν^{-2} QSO source evolution	65	
Yuksel *et al.* (2007) [67]	E_ν^{-2} GRB source evolution	100	
Kotera *et al.* (2010) [68]	Protons, SFR1 evolution	7.3	0.46 (0.64)
Kotera *et al.* (2010) [68]	Protons, GRB2 evolution	9.0	0.48 (0.67)
Kotera *et al.* (2010) [68]	Protons, FRII evolution	48	2.9 (4.0)
Yoshida *et al.* (1993) [69]	$m=4$, $z_{max}=4$	34	2.0 (2.8)
Ahlers *et al.* (2010) [70]	$E_{min}=10^{10}$ GeV (best fit)	26	1.5 (2.1)
Ahlers *et al.* (2010) [70]	$E_{min}=10^{10}$ GeV (maximal)	58	3.1 (4.3)
Kotera *et al.* (2010) [68]	Mixed composition	7.4	
Kotera *et al.* (2010) [68]	Pure Iron	2.5	
Ave *et al.* (2005) [71]	Pure Iron, $m=4$, $z_{max}=1.9$	18	
Olinto *et al.* (2011) [42]	Pure Iron, $E_{max}/Z=10^{11}$ GeV	0.097	
Aartsen *et al.* (2014) [24]	$E_\nu^{-2.3}$ IceCube best fit	2.8	
Fang *et al.* (2013) [72]	Young pulsar sources	43	

$$dN(E) = \frac{\phi(E)\epsilon V_{eff}\Omega t_{live}}{L_{int}} dE \tag{17}$$

$$E^2\phi(E) \leq \frac{2.3 \cdot E \cdot L(E)}{\ln 10 \epsilon V_{eff}\Omega t_{live}} \tag{18}$$

Neutrino Sensitivity

Neyman UL, 1937

Feldman-Cousins (1998) ordering principle that restricts confidence intervals to frequentist coverage, given the number of observations and expected background events.

$$P(n \leq N) = \sum_{i=0}^{N} P(i|(\lambda + b)) \quad (19)$$

$$P(n \leq 0; b = 0) = \exp(-\lambda) \rightarrow \quad (20)$$

$$\lambda = -\ln P \quad (21)$$

$$\lambda = 2.3 \;\; 90\% c.l. \quad (22)$$

To set a limit, we determine the energy (decade bins) that minimizes eq. 14.

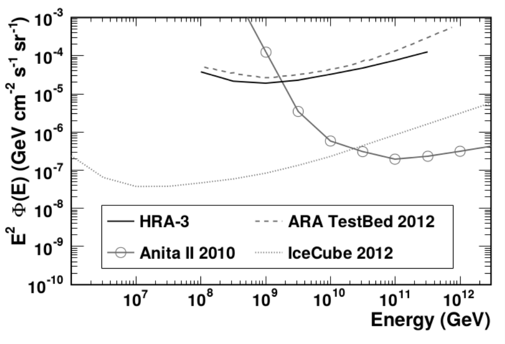

Quote of the limit

A model-independent 90% confidence-level Neyman upper limit is placed on the all-flavor, $\nu + \bar{\nu}$ flux in a sliding decade-wide energy bin. The limit reaches a minimum of 1.9×10^{-23} $\mathrm{GeV}^{-1}\mathrm{cm}^2\mathrm{s}^1\mathrm{sr}^1$ in the $10^{8.5} - 10^{9.5}$ GeV energy bin.

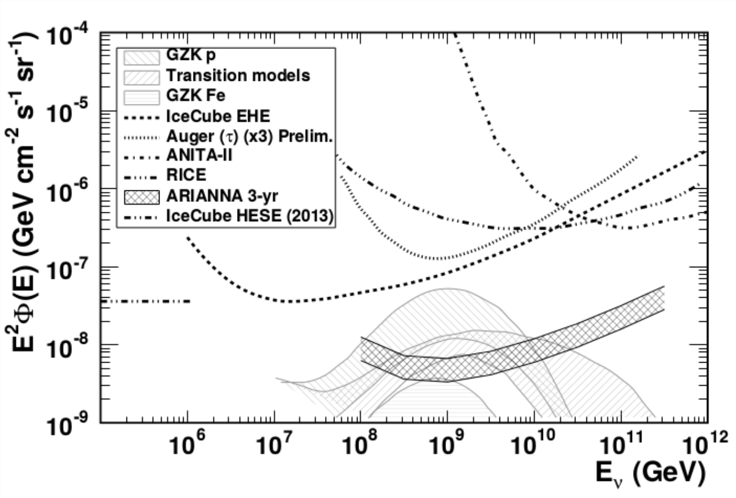
GZK p
Transition models
GZK Fe
IceCube EHE
Auger (τ) (x3) Prelim.
ANITA-II
RICE
ARIANNA 3-yr
IceCube HESE (2013)
E²Φ(E) (GeV cm⁻² s⁻¹ sr⁻¹)
10⁻⁴
10⁻⁵
10⁻⁶
10⁻⁷
10⁻⁸
10⁻⁹
10⁶
10⁷
10⁸
10⁹
10¹⁰
10¹¹
10¹²
E_ν (GeV)

CONCLUSION

I. UHE Neutrinos, Askaryan Effect
   A. Guaranteed neutrino signal from deep space
II. Deployed Hardware
   A. ARIANNA is online, taking data
III. Ice
   A. Improved understanding of ice effects
IV. System Response
   A. Fully modeled
V. Data Analysis
   A. Relatively simple waveform analysis, few man-made backgounds
VI. Neutrino Sensitivity
   A. Significant signal compared to projected thermal backgrounds

Bibliography I

I. Salamida, Francesco. *Update on the measurement of the CR energy spectrum above* 10^{18} *eV made using the Pierre Auger Observatory*. Proceedings of the 32nd Intl. Cosmic Ray Conf., Beijing, China (2011).

II. Barwick, S.W. *et al.* (ARIANNA). *A First Search for Cosmogenic Neutrinos with the ARIANNA Hexagonal Radio Array. Accepted for publication in J. Astrop. Phys.*

III. Ahlers, M., *et al. GZK neutrinos after the Fermi-LAT diffuse photon flux measurement.* J. Astrop. Phys., **34**, p. 106-115 (2010)

IV. Aartsen, M.G., *et al.. Probing the origin of cosmic rays with extremely high energy neutrinos using the IceCube Observatory*. Phys. Rev. D, **88**, p. 112008 (2013).

V. Hanson, J.C. *et al.* (ARIANNA). *Radar Absorption, Basal Reflection, Thickness, and Polarization Measurements from the Ross Ice Shelf. Accepted for publication in J. of Glaciol.*

VI. Reed, C. *et al.* (ARIANNA). *Performance of the ARIANNA Neutrino Telescope Stations*. Proceedings of the 33rd Intl. Cosmic Rays Conf., Rio de Janeiro, Brazil (2013).

VII. Hanson, J.C. *et al.* (ARIANNA). *Time-domain response of the ARIANNA detector*. J. of Astrop. Phys. **62** p. 139-151 (2015).

VIII. Kleinfelder, S. *et al.* (ARIANNA). *Design and Performance of the ARIANNA Hexagonal Radio Array Systems*. (*submitted to Nucl. Inst. Meth., A*).

IX. Dookayka, K. *Characterizing the Search for Ultra-High Energy Neutrinos with the ARIANNA Detector*, Ph.D. dissertation, University of Californa, Irvine (2011).

BACKUP SLIDES

Effect of Temperature on SST

The SST requires bias voltage and trigger threshold voltages to remain stable. Temperature instabilities cause observable trigger rate shifts, for a few mV drift.

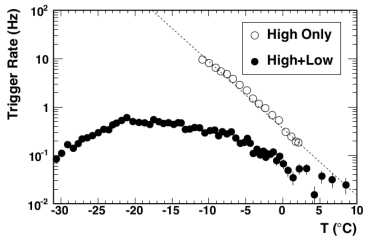

Double-sided threshold

The double threshold mitigates the effect, as long as the noise distribution is symmetric.

Verification of SST performance

By reflecting an RF pulse (100-1000 MHz) through the ice shelf, from the ocean, and back to the SST detector, we can match the SST recording to an oscilloscope.

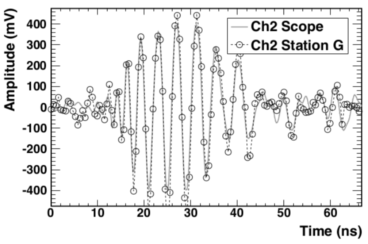

Realistic signal

The broadband nature of this pulse is similar to the expected neutrino signal, meaning the SST is capable of recording it.

I. Ice
   A. Completed Research
      i. Ice thickness
      ii. RF Absoprtion of ice
      iii. Reflection coefficient
      iv. Polarization preservation

$$\frac{\langle L \rangle}{\langle L_0 \rangle} = \left(1 + \frac{\langle L_0 \rangle}{2d_{ice}} \ln R\right)^{-1} \quad (23)$$

ν (GHz)	$\langle L_0 \rangle$ (m)	$\langle L \rangle$ (m)	(dB/km)	$\epsilon'' \times 10^3$	$\nu \tan\delta \times 10^4$
0.100	432	449	19.3	3.8	1.2
0.175	467	487	17.8	2.0	1.1
0.250	457	476	18.2	1.4	1.1
0.325	422	438	19.8	1.2	1.2
0.400	408	423	20.5	1.0	1.3
0.475	366	378	23.0	0.95	1.4
0.550	349	360	24.1	0.86	1.5
0.625	363	375	23.2	0.72	1.4
0.700	331	341	25.5	0.71	1.6
0.775	310	319	27.2	0.69	1.7
0.850	320	329	26.4	0.61	1.6
Ave.	380 ± 16	400 ± 18	22 ± 1	1.3 ± 0.3	1.37 ± 0.06

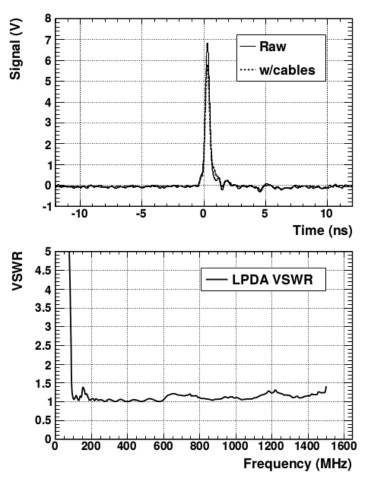

Signal (V)
Raw
w/cables
Time (ns)
VSWR
LPDA VSWR
Frequency (MHz)

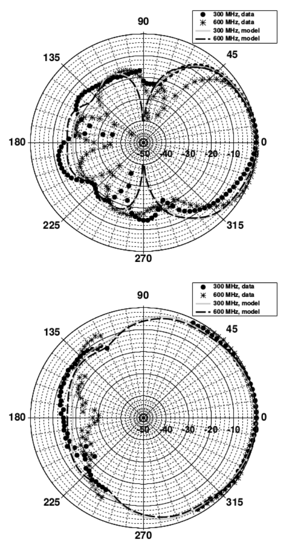

300 MHz, data
600 MHz, data
300 MHz, model
600 MHz, model
90
135
45
180
0
225
315
270
-50
-40
-30
-20
-10
300 MHz, data
600 MHz, data
300 MHz, model
600 MHz, model
90
135
45
180
0
225
315
270
-50
-40
-30
-20
-10

Cosmic Ray sensitivity

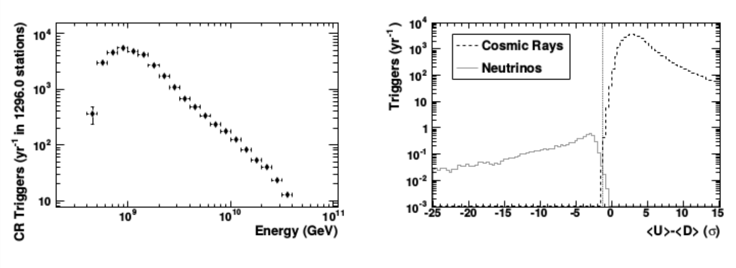

Cosmic ray EAS generate RF as well

We use CoREAS to generate generic UHECR pulses, and convolve with front (down) and back (up) lobes of LPDA response.

CoREAS configuration - details matter

- CR p^+: $10^{8.4}$-$10^{10.5}$ GeV are simulated by Corsika, QGSJetII-04 hadronic model, track up-going particles
- Event weighted by measured CR flux
- (Left): 3 of 8 downward facing antennas, 4σ trigger
- (Right): Use 2 of 8 antennas facing up, 45°, as veto-channels

Angular reconstruction. (Dookayka, 2011), (Reed, 2013)

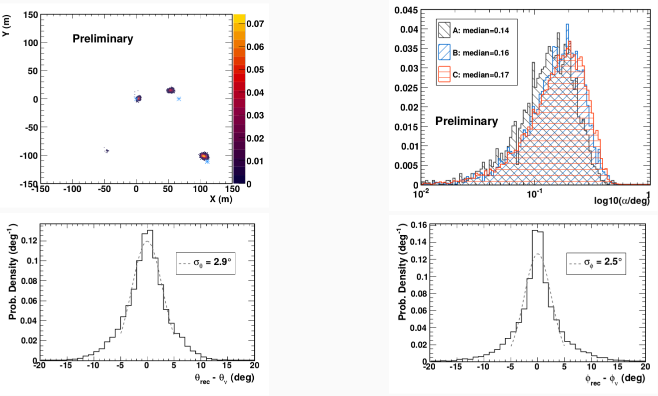

Upper left: pulser location reconstruction. Upper right: pulser angle reconstruction. Lower left: ν zenith reconstruction. Lower right: ν azimuth reconstruction.